Viscoelastic Properties of Binary Blends of Linear Polystyrenes: Further Examination of Constraint Release Models

Hiroshi Watanabe,* Manabu Yamazaki, Hirotsugu Yoshida, and Tadao Kotaka

Department of Macromolecular Science, Faculty of Science, Osaka University, Toyonaka, Osaka 560, Japan

Received March 13, 1991; Revised Manuscript Received May 21, 1991

ABSTRACT: The viscoelastic behavior of probe polystyrene (PS) chains in PS/PS blends was compared with the predictions of the so-called CICR and CDCR models for a combined constraint release (CR) plus reptation process. In the CICR model, the CR rate constant was assumed to be independent of the probe chain configuration. On the other hand, in the CDCR model, the CR process was assumed to proceed through configuration-dependent Rouse dynamics. In the eigenfunction expansion procedure of this model for *viscoelastic* relaxation, only diagonal Rouse eigenfunctions were used to evaluate the relaxation rate due to CR. This approximation was referred to as the diagonal-dominance approximation (DDA). As the matrix molecular weight M_S approached the probe molecular weight M_L, the M_S dependence of the relaxation time of the probe chain became gradually weaker, and the terminal mode distribution became narrower. Such behavior was much better described by the CDCR model than by the CICR model. This indicated the configuration dependence to be essential for actual CR processes. However, even for the CDCR model, agreements with the data were poor at short time scales, as most clearly seen in the CR-dominant regime ($M_L \gg M_S$). In that regime, the CDCR model with DDA was reduced to a pure CR model rigorously using Rouse dynamics (without DDA) and was found to *overestimate* fast viscoelastic modes. Thus, Rouse dynamics was valid as the actual CR dynamics only at long time scales. This in turn suggested that reasonably good agreements between the slow viscoelastic data and the present CDCR model in the entire range of M_S may be related to DDA used in the model. For M_S not much smaller than M_L, DDA *underestimated* fast viscoelastic modes and seemed to cancel to some extent the *overestimation* for those modes due to use of Rouse dynamics in the model.

I. Introduction

Entanglements exert a profound effect on slow dynamics of condensed systems of long polymer chains.[1] The dynamic behavior of such systems is often interpreted in terms of a generalized tube model.[2,3] For entangled linear chains, this model considers that the reptation mechanism is competing with some additional mechanisms such as contour length fluctuation[3,4] and constraint release[3,5,6] (CR) that are not accounted for in the original Doi–Edwards model.

Viscoelastic[7-12] as well as diffusion[13,14] experiments on binary blends of long and short monodisperse chains (with molecular weights M_L and M_S, respectively) established the importance of the CR mechanism under certain *extreme* conditions: For the long chain that is *dilute* in a blend and entangled only with *much shorter* matrix chains, the slow relaxation was dominated by the CR mechanism that led to a Rouse-like behavior with a characteristic time $\propto M_L^2 M_S^3$. However, the experiments also revealed that the CR dominance no longer holds as M_S approaches M_L. To describe the behavior for cases with $M_S \to M_L$ in terms of a generalized tube model, competition of CR and reptation has to be considered.

For the above competition, two types of models, referred to as the configuration-dependent and configuration-independent constraint release (CDCR and CICR) models, can be formulated.[15] In these models, the CR dynamics is incorporated in different ways. Watanabe and Tirrell[15] made a preliminary comparison for the two models with experiments[7-12] and suggested that there was better agreement with the CDCR model than with the CICR model. They also suggested, however, the necessity for more extensive comparison of the models with experiments for $M_S \to M_L$ so that the binary blend dynamics could be better understood.[15]

To further investigate the binary blend dynamics concerning the competition between CR and reptation mechanisms, we have conducted an extensive examination of viscoelastic and dielectric properties of probe chains in blends with $M_S \to M_L$. In the dielectric tests,[16,17] we examined the behavior of probe *cis*-polyisoprene (PI) chains uniformly mixed and entangled only with polybutadiene (PB) matrices. *cis*-PI chains have dipoles *parallel* to the chain contour and thus exhibit slow dielectric relaxation that reflects their global motion.[18] The PB chains, without such dipoles, are dielectrically inert at long time scales. This enabled us to easily observe the behavior of a small amount of PI chains in PB matrices.[16] The behavior was compared with predictions of the CICR and CDCR models in our recent paper.[17]

In this paper, we present results of viscoelastic tests on binary blends of linear polystyrenes (PS). In section III, we briefly summarize the features of the CICR and CDCR models for viscoelastic relaxation.[15] In section IV, we quantitatively compare viscoelastic data obtained in this and previous studies with the predictions of the two models. Finally, in section V, we discuss the limitations of the models in relation to the results of the previous dielectric study on probe PI chains in PB matrices.[16,17]

II. Experimental Section

Measurements. Linear viscoelastic measurements were made with a laboratory rheometer (IR-200, Iwamoto Seisakusho). The characteristics of PS samples are summarized in Table I. The sample code number represents the molecular weight in units of 1000. The L1810 sample was used as the long-chain component, and the remainder as the matrix. As shown in Table I, all PS samples had narrow molecular weight distributions ($M_w/M_n \leq 1.1$). The details of sample preparation, characterization, and measurements were described elsewhere.[7-9,12]

All blends examined in this study contained 40 vol % of a plasticizer, dioctyl phthalate (DOP), and the content of polymeric

0024-9297/91/2224-5573$02.50/0 © 1991 American Chemical Society

Table I
Characteristics of Linear Polystyrene Samples

code	$10^{-3}M_w$	M_w/M_n
L71	71.4	1.06
L124[a]	124	1.05
L172[a]	172	1.07
L315[a]	315	1.07
L775[a]	775	1.01
L1810	1810	1.10

[a] From Tosoh Co.

components was always $\phi_p = 60$ vol %. We mostly examined the behavior of so-called *dilute* blends, in which the long probe PS chains were a dilute component (with the content $\phi_L = 1.5$ vol %) and entangled only with the matrix PS. For one particular series of blends composed of L1810 and L71 chains, we extensively varied ϕ_L, while keeping $\phi_p = \phi_L + \phi_S = 60$ vol %, to examine the onset of entanglements between long PS chains. The characteristic molecular weight for entanglement $M_e = M_e^\circ/\phi_p$ is 52×10^3 for $\phi_p = 60$ vol %. ($M_e^\circ = 31 \times 10^3$ is the M_e for bulk PS.) Therefore, all matrix chains (with $M \geq 71.4 \times 10^3$) used in this study were long enough to entangle with the probe chain (L1810). The time–temperature superposition principle was used and all viscoelastic data were reduced at $T_r = 71$ °C. The shift factor a_T was well represented by the previously reported WLF equation:[8,9,12] $\log a_T = -6.74\,(T - T_r)/(133.6 + T - T_r)$. The free-volume fraction at 71 °C is $f_r = 0.0644$ for the PS/PS/DOP blends with $\phi_p = 60$ vol %.[12]

Data Analysis. In a blend with small ϕ_L ($\ll\phi_S$; ϕ_S = short-chain content), the behavior of the short chains is hardly affected by the long chains. As explained in previous papers,[7,8,12] the dynamic modulus $G^*_{L,B} = G'_{L,B} + iG''_{L,B}$, viscosity $\eta_{L,B}$ ($=G''_{L,B}/\omega|_{\omega\to 0}$), elastic coefficient $A_{L,B}$ ($=G'_{L,B}/\omega^2|_{\omega\to 0}$), and compliance $J_{L,B}$ of the long probe chains *placed in such a blend* are evaluated by

$$G^*_{L,B}(\omega) = G^*_B(\omega) - (\phi_S/\phi_p)G^*_{S,m}(\omega) \quad (1)$$

$$\eta_{L,B} = \eta_B - (\phi_S/\phi_p)\eta_{S,m} \quad (2a)$$

$$A_{L,B} = A_B - (\phi_S/\phi_p)A_{S,m} \quad (2b)$$

$$J_{L,B} = A_{L,B}/(\eta_{L,B})^2 \quad (2c)$$

On the right-hand side of eqs 1–2b the subscript S,m stands for the experimentally determined quantities for the *monodisperse* system of the *short* matrix chains, and B, those for the *blend*, with ϕ_p being the same for both systems. Note that the product $J_{L,B}\eta_{L,B}$ represents the *weight-average* relaxation time of the long chains in the blend.[8,9,12]

In a blend with large ϕ_L, the relaxation of the short chains is in general retarded by the long chains. In principle, we have to consider this retardation effect to evaluate the quantities for the long chains from those for the blend as a whole and the matrix.[7,8] However, when the retardation due to the long chains became prominent for large ϕ_L, the short chains hardly contributed to the slow relaxation of the blends examined; e.g., $\eta_B \gg (\phi_S/\phi_p)\eta_{S,m}$ and $A_B \gg (\phi_S/\phi_p)A_{S,m}$ in eqs 2a and 2b. Thus, eqs 1–2c were used also for the blends with large ϕ_L to evaluate the quantities for the *slow* relaxation of the long chains.

III. Theory

1. General. We consider a blend of long and short primitive chains (hereafter referred to as chains) composed of N_L and N_S entanglement segments (referred to as segments). The long and short chains considered here are chemically identical, and their segmental friction coefficient is denoted commonly by ζ_0. The content of the long chain in the blend is ϕ_L, and that for the short chain, ϕ_S ($=\phi_p - \phi_L$; ϕ_p = total polymer content in the blend). ϕ_L is assumed to be small so that the long chains entangle only with the short matrix chains.

A viscoelastic relaxation of the long (*probe*) chain reflects its orientation relaxation.[2,3] After imposition of a small shear strain γ at time $t = 0$, an orientation function $S(n,t)$ of the probe chain decays with time. The function $S(n,t)$, representing an anisotropy of the bond orientation, is defined (for a shear component) by[2,3]

$$S(n,t) = (1/a^2)\langle u_x(n,t)\, u_y(n,t)\rangle \quad (3)$$

Here, a is the segment size and $u_\xi(n,t)$ is the $\xi(=x$ and $y)$ component of the nth bond vector of the probe chain at time t. Assuming the Doi–Edwards initial condition,[2,3] we have for $\gamma \ll 1$

$$S(n,0) = S_0 = 4\gamma/15 \quad (0 < n < N_L) \quad (4)$$

The boundary condition for $S(n,t)$, representing a random orientation at chain ends, is given by[2,3]

$$S(n,t) = 0 \quad \text{for } n = 0, N_L \quad (5)$$

The relaxation modulus $G_{L,B}(t)$ of the probe chains with the content ϕ_L is related to $S(n,t)$ as

$$G_{L,B}(t) = (\phi_L/\phi_p)G_N\mu_{L,B}(t) \quad (6)$$

with

$$\mu_{L,B}(t) = \frac{1}{N_L S_0}\int_0^{N_L} S(n,t)\, dn \quad (7)$$

Here, G_N is the plateau modulus of the monodisperse system with polymer content ϕ_p, and $\mu_{L,B}(t)$, the reduced relaxation modulus (with $\mu_{L,B}(0) = 1$) for the probe chain in the blend. All linear viscoelastic quantities of the probe chain can be calculated from $G_{L,B}(t)$.

We assume that the probe chain can relax through both reptation and constraint release (CR) mechanisms and calculate $S(n,t)$ and $\mu_{L,B}(t)$. In general, the CR mechanism is considered to induce a Rouse-like motion at long time scales for the tube confining the probe chain.[3,5,6] Thus, for slow CR processes, the tube may be regarded as a Rouse chain composed of N_L segments with the friction coefficient ζ_t. Specifically, we use the local jump scheme of Graessley[3] to write ζ_t as

$$\zeta_t = \frac{12\Lambda(z)\zeta_0 N_S^3}{\pi^2} \quad (8)$$

where $\Lambda(z) = (\pi^2/12)^z/z$ is a constant determined by the number z of local jump gates per entanglement point. The number z may depend on the chemical feature of the chains but should not depend on N_L and N_S.

For combined CR and reptation processes, two types of models can be formulated according to the expression for changes of $S(n,t)$ due to CR: One is the so-called configuration-independent CR (CICR) model, and the other, the configuration-dependent CR (CDCR) model. The features of these models (for $N_L \gg 1$; a continuous limit) were extensively discussed by Watanabe and Tirrell.[15] Here, for convenience for later discussion, we briefly summarize the features.

2. CICR Model.[19] This model assumes that the constraint release (CR) process takes place uniformly at any time throughout the chain contour, *irrespective* of the chain configuration. This assumption leads to a time evolution equation for $S(n,t)$ of the probe chain:[15]

$$\frac{\partial S(n,t)}{\partial t} = D_c\frac{\partial^2 S(n,t)}{\partial n^2} + k_{CR}(t)\, S(n,t) \quad (9)$$

Here, D_c is the curvilinear diffusion coefficient of the probe

chain:

$$D_c = kT/a^2 N_L \zeta_0 \tag{10}$$

$k_{CR}(t)$ is the n-independent rate constant for a viscoelastic CR process assumed in the CICR model:[15]

$$k_{CR}(t) = \frac{1}{\mu_{CR}(t)} \frac{d\mu_{CR}(t)}{dt} \tag{11}$$

with

$$\mu_{CR}(t) = \frac{1}{N_L} \sum_{q=1}^{N_L} \exp[-2D_t \lambda_q^2 t] \quad (N_L \gg 1) \tag{12}$$

and

$$D_t = \frac{3kT}{a^2 \zeta_t} = \frac{\pi^2 N_L D_c}{4\Lambda(z) N_S^3}, \quad \lambda_q = \frac{q\pi}{N_L} \quad (q = 1, 2, ..., N_L) \tag{13}$$

With the initial and boundary conditions, eqs 4 and 5, eq 9 can be solved to give $S(n,t)$, from which $\mu_{L,B}(t)$ is obtained as[15]

$$\mu_{L,B}(t) = \mu_{CR}(t)\, \mu_{rep}(t) \tag{14}$$

Here, $\mu_{rep}(t)$ is the reduced reptation function given by

$$\mu_{rep}(t) = \sum_{p=odd} \frac{8}{p^2 \pi^2} \exp[-D_c \lambda_p^2 t] \tag{15}$$

It should be noted that the CICR model leads to $\mu_{L,B}$ factorized into pure reptation (μ_{rep}) and pure CR (μ_{CR}) functions (cf. eq 14). In some models[3,5,20] for combined CR plus reptation processes, an *independence* of CR and reptation is assumed in a sense that the probability of survival of initial memory for the combined process is given by a product of probabilities for *pure* CR and *pure* reptation processes. Because μ represents this probability for viscoelastic relaxation, the above assumption directly leads to the factorized form of μ, as deduced also from the CICR model (cf. eq 14). The equivalence of the class of models[3,5,20] assuming the *independence in the above sense* and the CICR model was discussed by Watanabe and Tirrell.[15]

3. CDCR Model. In general, CR processes are considered to proceed through the Rouse dynamics. Then, their rate constant should be dependent on the chain configuration, i.e., on both n and t. From this point of view, Watanabe and Tirrell discussed a problem of the CICR model and proposed a configuration-dependent constraint release (CDCR) model.[15] The CDCR model assumes that CR and reptation steps successively take place during a short period of time and uses eigenfunction expansion to describe changes in the configuration of the probe chain.

For the time evolution of $S(n,t)$ with the boundary condition, eq 5, the eigenfunctions, f_{pq}^{CR} and f_p^{rep}, for the Rouse (CR) and reptation steps are given by

$$f_{pq}^{CR} = \sin(\lambda_p n) \sin(\lambda_q n) \quad (p, q = 1, 2, ..., N_L) \tag{16}$$

$$f_p^{rep} = \sin(\lambda_p n) \quad (p = 1, 2, ..., N_L) \tag{17}$$

To analytically solve the problem for $S(n,t)$, Watanabe and Tirrell[15] used only the diagonal Rouse functions, f_{qq}^{CR}, and evaluated the decay of $S(n,t)$ during the CR step. This approximation was referred to as the diagonal-dominance approximation (DDA).

For $N_L \gg N_S$ (in a CR-dominant regime), the CDCR model with DDA is identical with a *pure* CR model that considers the relaxation due only to CR and *rigorously* uses Rouse dynamics as the CR dynamics. However, if N_L and N_S are not very different, the decay of $S(n,t)$ for the CR step evaluated with DDA is slower than that with rigorous Rouse dynamics.[21] In other words, DDA *underestimates* the viscoelastic relaxation as compared to rigorous Rouse dynamics. This feature of DDA is discussed later in section V in relation to experimental results in a CR-dominant regime (cf. Figure 13).

On the basis of DDA, Watanabe and Tirrell expanded $S(n,t)$ with respect to f_{qq}^{CR} (eq 16) and f_p^{rep} (eq 17) to evaluate the amplitudes of these eigenfunctions, allowed the amplitudes to decay during the CR and reptation steps according to the respective dynamics, and obtained a time evolution equation:[15]

$$\frac{1}{D}\frac{\partial S(n,t)}{\partial t} = \frac{\partial^2 S(n,t)}{\partial n^2} - w\left[\int_0^{N_L} dm\, Q(m) \frac{\partial^2 S(m,t)}{\partial m^2} - \left[\frac{\partial S(m,t)}{\partial m}\right]_{m=0}^{m=N_L}\right] \tag{18}$$

with

$$D = D_c + {}^1/_2 D_t, w = D_t/D,$$

$$Q(m) = (1/N_L) \sum_{q=1}^{N_L} \cos(2\lambda_q m) \tag{19}$$

In the above eigenfunction expansion for the CR step, the Rouse eigenfunctions f_{qq}^{CR} were used for all mode orders ($q = 1, 2, ..., N_L$). In other words, the model uses Rouse dynamics as the CR dynamics at any time scale (but in an approximate way because of DDA). We discuss this point later in section V.

With eqs 4 and 5, eq 18 can be solved for $N_L \gg 1$ to give $S(n,t)$, from which $\mu_{L,B}(t)$ of the probe chain is calculated as[15]

$$\mu_{L,B}(t) = \sum_{p=1}^{N_L} B_p' \exp[-D(2\theta_p/N_L)^2 t] \tag{20}$$

with

$$B_p' = \frac{b_p'}{\sum_{k=1}^{N_L} b_k'}, \qquad b_p' = \frac{\cos^2 \theta_p}{w(2N_L + 1) + (2 - w)\cos^2 \theta_p},$$

$$p = 1, 2, ..., N_L \tag{21}$$

The eigenvalue θ_p is determined by the equation

$$\tan \theta_p = -\frac{2}{2N_L + 1} \frac{D_c}{D_t} \theta_p \tag{22}$$

As seen in eq 22, θ_p is determined by N_L and also by the ratio D_t/D_c ($\propto N_L/N_S^3$). Thus, changes in the relative contribution of the CR and reptation mechanisms (represented by this ratio) lead to changes in the eigenvalue problem for $S(n,t)$. In this connection, it should be noted that $\mu_{L,B}(t)$ deduced from the CDCR model (eq 20) does not have a factorized form, as is essentially different from $\mu_{L,B}(t)$ for the CICR model (eq 14).

4. MWD of Probe Chains. The CICR and CDCR models explained in the previous sections are the models for *monodisperse* probe chains. However, the probe chains used have narrow but finite molecular weight distributions (MWD) that were not considered in the previous work.[15] In this paper, to make a correction for small MWD, we used a MWD function of the probe chain determined by gel permeation chromatography (GPC) to calculate $\mu_{L,B}(t)$. To this end, we divided the MWD function into f

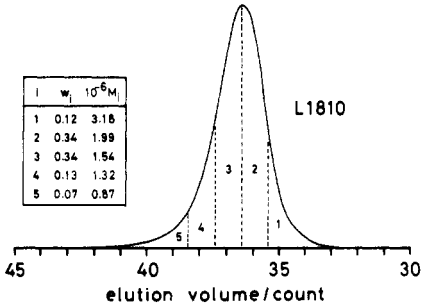

Figure 1. Gel permeation chromatogram (GPC) of L1810 divided into $f = 5$ fractions. The width of the GPC section is $\Delta \log M = 0.11$ (1 count of elution volume) for the middle fractions ($i = 2$–4), and the boundary between the second and third fractions is located at the GPC peak. The tails of the GPC are assigned to the end fractions ($i = 1, 5$). The weight-average molecular weight of each fraction was used as M_i.

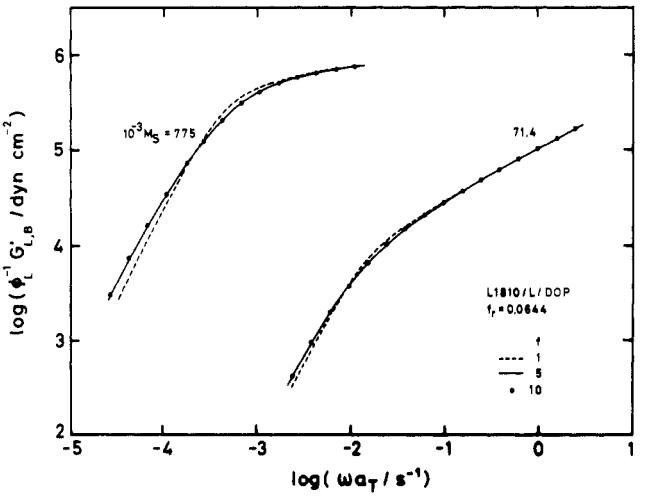

Figure 2. $G'_{L,B}/\phi_L$ curves of the L1810 probe chain in L71 and L775 matrices calculated from the CDCR model with MWD. The model parameters are the same as those used in Figures 7–11. The dashed curves, solid curves, and circles, respectively, indicate the $G'_{L,B}/\phi_L$ curves calculated for the MWD function of L1810 divided into $f = 1$, 5, and 10 fractions.

fractions and evaluated the weight fraction w_i and molecular weight M_i of the ith fraction. As an example, Figure 1 shows the GPC trace of the L1810 probe chain divided into $f = 5$ fractions. With the w_i and M_i thus evaluated, we calculated the reduced relaxation modulus of the probe chain as

$$\mu_{L,B}(t) = \sum_i w_i \mu(t;M_i) \tag{23}$$

Here, $\mu(t;M_i)$ for the ith fraction is given by eq 14 for the CICR model, and by eq 20 for the CDCR model.

Figure 2 shows $G'_{L,B}/\phi_L$ curves of the L1810 probe chain calculated for the MWD function divided into $f = 1$, 5, and 10 fractions. For $f = 10$, each fraction for $f = 5$ (cf. Figure 1) was further divided into two fractions. As can be seen in Figure 2, the viscoelastic quantities of the L1810 chain calculated for $f = 5$ and 10 are very close to each other but those for $f = 1$ (without MWD) are different in particular when the matrix molecular weight M_S is not much smaller than M_L. This result was found also for other probe chains with small MWD ($M_w/M_n < 1.1$) examined in the previous work.[7-12] Thus, in the next section, the viscoelastic quantities calculated for $f = 5$ are compared with the experimental data.

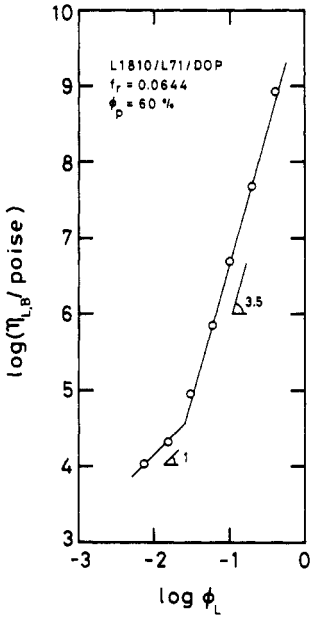

Figure 3. ϕ_L dependence of viscosity of the probe L1810 chains in blends with L71 at 71 °C.

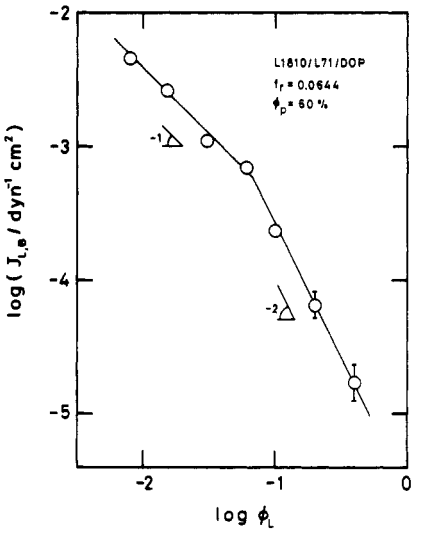

Figure 4. ϕ_L dependence of compliance of the probe L1810 chains in blends with L71 at 71 °C.

IV. Results

1. Onset of Entanglements between Probe Chains. To examine at what ϕ_L entanglements between probe chains become significant, we carried out viscoelastic measurements on L1810/L71 blends with ϕ_L ranging from 0.8 to 40 vol % and $\phi_p = 60$ vol %. The molecular weights of the long and short chains were very different in those blends so that we were able to clearly observe the onset of such entanglements. The viscosity $\eta_{L,B}$ and compliance $J_{L,B}$ of the long chains that characterize the terminal relaxation were evaluated by eqs 2a–c. Figures 3 and 4 shows the ϕ_L dependence of these quantities.

As seen in Figure 3, the ϕ_L dependence of $\eta_{L,B}$ exhibits a crossover from $\eta_{L,B} \propto \phi_L$ to $\eta_{L,B} \propto \phi_L^{3.5}$ as ϕ_L exceeds a critical value, $\phi_{c,L} = 2$–2.5 vol %, for the onset of probe–probe (L–L) entanglements. The $\phi_{c,L}$ value is in the vicinity of the critical value,[7] $M_c^\circ/M_L = 1.8$ vol %, expected for solutions of L1810 chains. In Figure 4, we find that the change in the ϕ_L dependence of $J_{L,B}$ due to L–L entanglements (from $J_{L,B} \propto \phi_L^{-1}$ to $J_{L,B} \propto \phi_L^{-2}$) takes place at ϕ_L somewhat larger than $\phi_{c,L}$ for $\eta_{L,B}$.[11] The CICR and CDCR models are applicable for the probe chains with ϕ_L

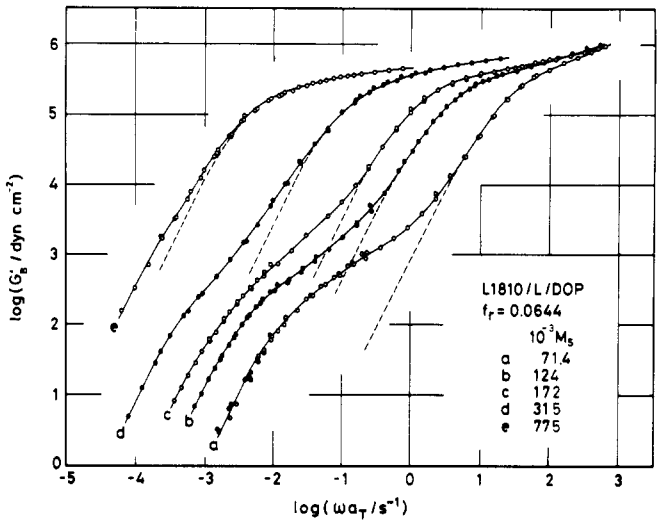

Figure 5. Comparison of the G' curves of the L1810/L/DOP dilute blends at 71 °C. For all blends, the content ϕ_L of the probe L1810 is 1.5 vol % ($<\phi_{c,L}$), and the total polymer content ϕ_p is 60 vol %. The dashed curves indicate the G' curves of the matrix PS in their monodisperse systems with ϕ_p = 60 vol %.

$< \phi_{c,L}$ that are entangling only with the matrix chains.

2. Behavior of Probe Chains in Dilute Blends. Figure 5 compares the frequency dependence of the storage moduli G'_B of *dilute* blends of the probe L1810 chain with various matrices as indicated. For all the blends, the content ϕ_p of the polymeric components (probe plus matrix) is 60 vol %, and the probe (L1810) chain content, ϕ_L = 1.5 vol % ($<\phi_{c,L}$; cf. Figure 3). The dashed curves indicate the behavior of the matrix chains in their monodisperse systems with ϕ_p = 60 vol %.

The relative contributions of the constraint release (CR) and reptation mechanisms to the behavior of the probe chain can be represented by the ratio $M_L M_e^2/M_S^3$ ($\propto D_t/D_c$), with M_e being the entanglement spacing. The minimum value of this ratio examined in Figure 5 (=2.2 × 10^{-3}) is smaller than that (=3.5 × 10^{-3}) in the previous work.[15] We can thus observe changes in the behavior of probe chains with decreasing CR contribution (with increasing M_S) more clearly in Figure 5 than in the previous work.

As seen in Figure 5, the blends exhibit slow and fast relaxation processes, the former due to the long probe chains and the latter mainly to the matrix chains. The relaxation of the probe chain is retarded first strongly and then rather weakly with increasing M_S. This behavior is characteristic of competition of CR and reptation, as found in the previous work.[8,12,15] We compare the relaxation time of the probe chain with the model predictions later in Figure 10.

Changes in the viscoelastic relaxation mode distribution of probe chains with increasing M_S are another important consequence of the competition of CR and reptation.[8,12,15] To examine such changes in the clearest fashion, we reduced the storage moduli $G'_{L,B}$ of the probe L1810 chain in various matrices by its content ϕ_L and shifted the $G'_{L,B}/\phi_L$ curves along the frequency axis by adequate factors λ so that their low-frequency tails (where $G'_{L,B} \propto \omega^2$) were superposed. The shape of the curves thus obtained is compared in Figure 6.

As seen in Figure 6, the $G'_{L,B}/\phi_L$ curves have almost the same shape and thus the relaxation mode distribution is almost the same for $10^{-3}M_S$ = 71.4 and 124. For these M_S ($\ll M_L$ = 1810 × 10^3), the CR mechanism is dominating the slow relaxation of the probe chain. With further increase in M_S, however, the terminal mode distribution

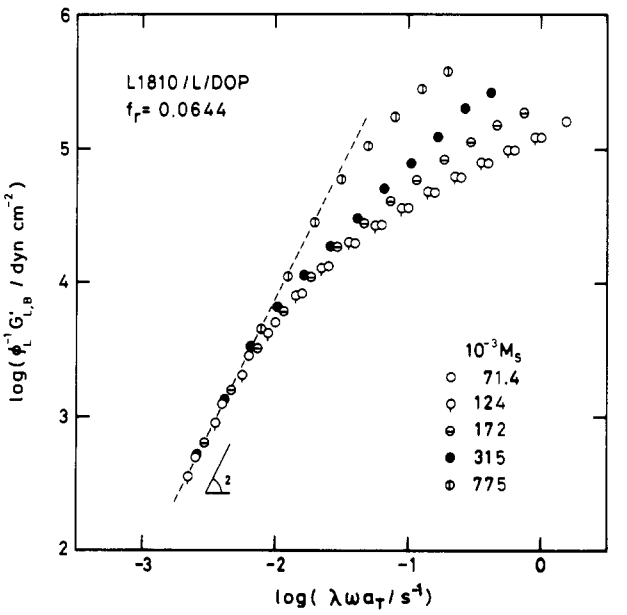

Figure 6. Comparison of the shape of $G'_{L,B}/\phi_L$ curves in the terminal region for the probe L1810 chain in the blends examined in Figure 5. Those curves are shifted along the frequency axis by adequate factors λ, so that their low-frequency tails are superposed.

of the probe chain becomes narrower, exhibiting steeper $G'_{L,B}/\phi_L$ curves at low ω. This behavior is compared with the prediction of the CICR and CDCR models later in Figure 9.

3. Comparison with the Models. The CICR and CDCR models involve the same set of parameters: the entanglement spacing M_e, the curvilinear diffusion coefficient of the probe chain D_c (eq 10), and the local jump gate number z that determines the tube segment mobility D_t (eq 13). M_e is evaluated from the plateau modulus G_N of monodisperse PS systems with PS content ϕ_p through the Doi–Edwards relation:[2]

$$M_e = \frac{4\rho\phi_p RT}{5G_N} \tag{24}$$

where ρ is the density of the system and RT has its usual meaning. D_c can be evaluated from G_N and the viscosity η_c of *nonentangled* PS having characteristic molecular weight M_c as[2,15]

$$D_c = \frac{M_c}{M_L}\frac{5G_N}{144\eta_c} \tag{25}$$

Finally, z is evaluated from a comparison of calculated and observed $G'_{L,B}$ in a *CR-dominant* regime for $M_L \gg M_S > M_c$. In this regime, the CICR and CDCR models lead to the *same* reduced relaxation modulus for a probe chain with small MWD (cf. eq 23):

$$\mu_{L,B}(t) = \sum_i w_i \mu_{CR}(t;M_i) \tag{26}$$

Here, the pure CR function for the ith fraction of the probe chain, $\mu_{CR}(t;M_i)$, is given by eq 12.

From a comparison of the calculated (eq 26) and measured $G'_{L,B}$ in the CR-dominant regime for L315 ($10^{-3}M_L$ = 315; ref 8), L1810 (this work), and L2810 ($10^{-3}M_L$ = 2810; ref 9) probe chains, we obtained z = 3. As shown with the solid curves in Figure 7, the models with M_L- and M_S-independent z value (=3) well describe the slow relaxation behavior of the three probe chains (circles). This z value is a little smaller than that (z = 3.5) evaluated in a previous paper,[15] because we have considered MWD

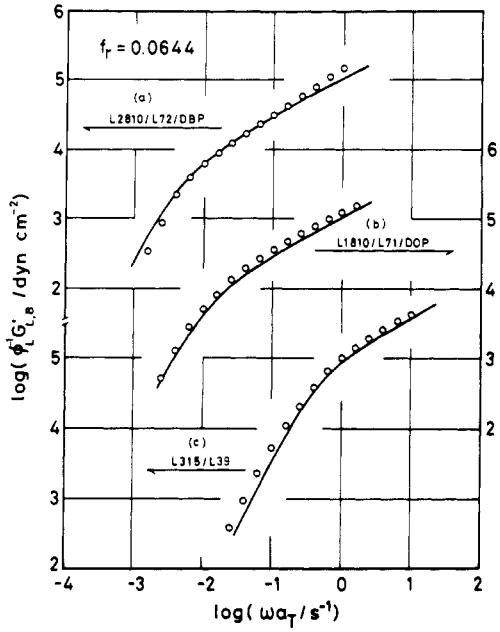

Figure 7. Comparison of the observed and calculated $G'_{L,B}/\phi_L$ curves at an isofriction state with $f_r = 0.0644$ for three probe PS chains entangled with much shorter matrix chains. For the data (circles) the reference temperature T_r (°C), $10^{-3}M_L$, $10^{-3}M_S$, ϕ_L, and ϕ_p (vol %) are (a) 54, 2810, 72.4, 1, and 60 for the L2810/L72/dibutyl phthalate (DBP) blend (from ref 9); (b) 71, 1810, 71.4, 1.5, and 60 for the L1810/L71/DOP blend (this work); and (c) 167, 315, 38.9, 5, and 100 (bulk) for the L315/L39 blend (from ref 8). The $G'_{L,B}/\phi_L$ curves calculated from the CDCR and CICR models were indistinguishable and are indicated with the solid curves.

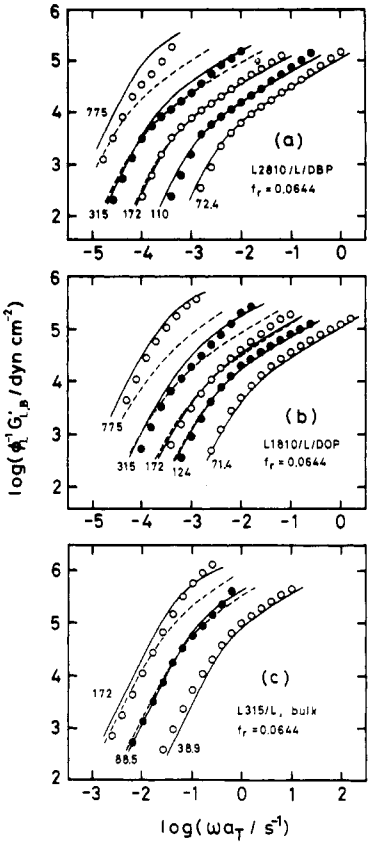

Figure 8. Comparison of the observed and calculated $G'_{L,B}/\phi_L$ curves at an isofriction state with $f_r = 0.0644$ for the three series of blends indicated. The numbers in the figure represent $10^{-3}M_S$. For the data (circles) T_r (°C), ϕ_L, and ϕ_p (vol %) are (a) 54, 1, and 60 for the L2810/L/DBP blends (from refs 9 and 12); (b) 71, 1.5, and 60 for the L1810/L/DOP blends (this work); and (c) 167, 5, and 100 (bulk) for the L315/L39 and L315/L89 blends and 167, 10, and 100 for the L315/L172 blend (from ref 8). The solid and dashed curves respectively, indicate the predictions of the CDCR and CICR models. The small MWD of the probe chains was incorporated in the calculation through eq 23.

and used the data for three different probe chains in the present evaluation of z.

Using the experimentally determined parameters, we calculated the viscoelastic quantities of the probe chains in various matrix chains. Figure 8 shows the observed and calculated $G'_{L,B}$ at low frequencies for three series of dilute blends as indicated. We note that the data (circles) for $M_S \to M_L$ are better described by the CDCR model (solid curves) than by the CICR model (dashed curves).

Figure 9 compares the terminal relaxation mode distribution of the L1810 probe chain (circles) with the model predictions. The observed and calculated $G'_{L,B}/\phi_L$ curves were shifted along the frequency axis so that their low-frequency tails were superposed, as was done in Figure 6. As seen in Figure 9, the predictions of the CICR and CDCR models for $M_S = 71.4 \times 10^3$ (in the CR-dominant regime) are indistinguishable (solid curve) and agree well with the data. However, for M_S not very different from M_L (=1810 $\times 10^3$), the mode distribution deduced from the CICR model (dashed curves) is significantly broader and the terminal intensity, smaller, than the experimental results. On the other hand, the CDCR model (solid curves) fairly well describes the distribution even for $M_S \to M_L$.

Figure 10 shows the dependence of the weight-average relaxation time, $J_{L,B}\eta_{L,B}$, of the probe PS chains examined in Figure 8 on matrix molecular weight M_S. The data (circles) obtained in this and previous work[8,9,12] are compared at an isofriction state with $f_r = 0.0644$. The solid and dashed curves, respectively, indicate the predictions of the CDCR and CICR models.

In Figure 10, we note that the relaxation time increases rapidly (in proportion to M_S^3) with increasing M_S if $M_S \ll M_L$ (see the data for the L2810 blends). With further increase in M_S ($\to M_L$), the relaxation time depends on M_S less significantly but still increases gradually, as most clearly seen for the L1810 blends. These results are better described by the CDCR model (solid curves) than by the CICR model (dashed curves).

Figure 11 shows the viscosity (η) data of *monodisperse* (narrow MWD) PS chains[7-9,11,12] at an isofriction state with $f_r = 0.0644$. To compare the data for $\phi_p = 100$ (bulk), 60, and 36.4 vol % in the same figure, η are plotted against a reduced molecular weight $\phi_p M$.[22] The dash–dot and dashed curves, respectively, indicate the predictions of the CDCR and CICR models with the parameters determined for the PS/PS blends (cf. eqs 24 and 25 and Figure 7). As found in the previous work,[15] the CDCR model *overestimates* while the CICR model *underestimates* η for high-M monodisperse PS chains.

Here, it is of interest to examine the models for polymer chains other than PS. Figure 12 compares the η data (circles) of monodisperse bulk *cis*-polyisoprenes (PI)[23] with the predictions of the CDCR (dash–dot curves) and CICR (dashed curves) models. The model parameters M_e and D_c were evaluated by eqs 24 and 25. Since data are not available for PI/PI dilute blends, we could not determine z but assumed reasonable z values (=3, 4, and 6) in the calculation. As seen in Figure 12, the CDCR and CICR models again over- and underestimate η for high-M PI chains. This result seems to be the case for various polymers with the characteristic molecular weight $M_c \cong 2M_e$, as were the cases for PS and PI.

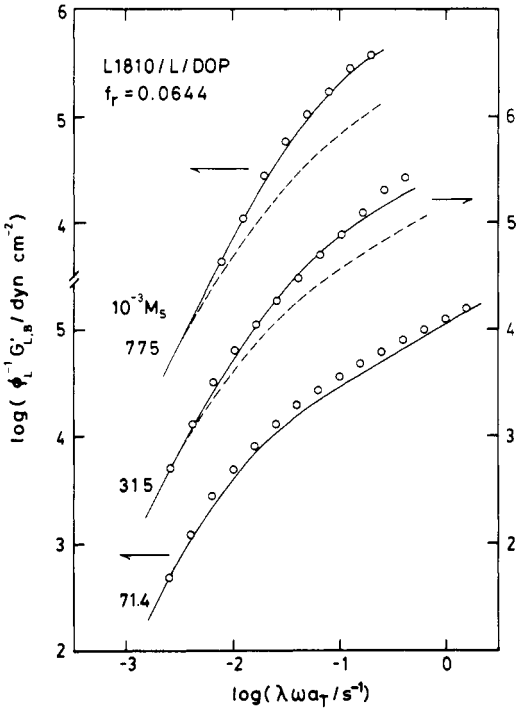

Figure 9. Comparison of the shape of $G'_{L,B}/\phi_L$ curves of the L1810 probe chains at 71 °C (circles) with predictions of the CDCR (solid curves) and CICR (dashed curves) models. For all blends, ϕ_p and ϕ_L are 60 and 1.5 vol %, respectively. The observed and calculated $G'_{L,B}/\phi_L$ curves are shifted along the frequency axis by adequate factors λ, so that their low-frequency tails are superposed.

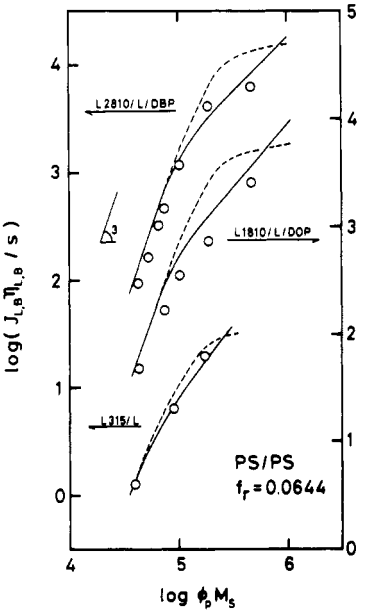

Figure 10. Comparison of observed (circles) and calculated weight-average relaxation time at an isofriction state with f_r = 0.0644 for the three probe chains examined in Figure 8. To compare the relaxation times for ϕ_p = 60 and 100 vol %, they are plotted against the reduced molecular weight of the matrix, $\phi_p M_S$. The solid and dashed curves, respectively, indicate the predictions of the CDCR and CICR models.

V. Discussion

1. Configuration Dependence of CR Processes. In Figures 8–10, we have found that the viscoelastic behavior of probe PS chains in dilute blends is certainly better described by the CDCR model than by the CICR model. In addition, the underestimation of viscosity by the CICR model for highly entangled monodisperse systems (cf.

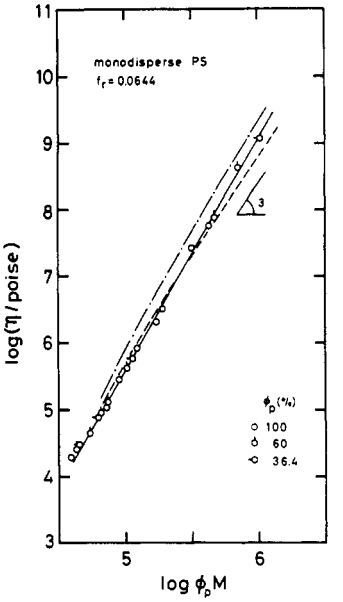

Figure 11. Comparison of observed[7-9,11,12] (circles) and calculated viscosity η of monodisperse PS at an isofriction state with f_r = 0.0644. The reference temperatures are 167, 71, 54, and 6 °C, respectively, for ϕ_p (in vol %) = 100 (bulk PS),[7,8,11] 60 (PS/DOP),[12] 60 (PS/DBP),[9,12] and 36.4 (PS/DBP).[9] To compare η for various ϕ_p in the same figure, η are plotted against reduced molecular weight $\phi_p M$, and a small correction for the intensity factor[22] was made. The dash–dot and dashed curves, respectively, indicate the prediction of the CDCR and CICR models with the parameters determined for PS/PS dilute blends.

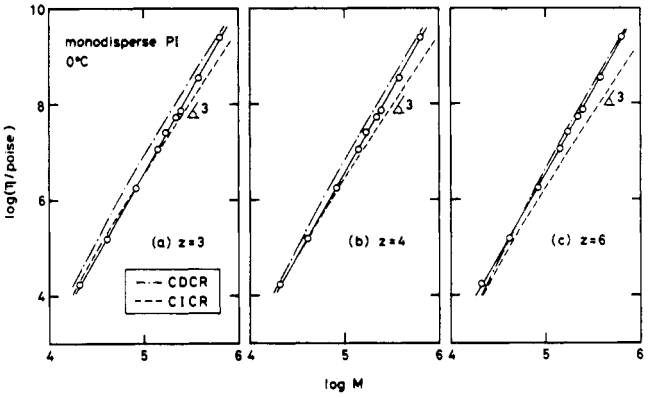

Figure 12. Comparison of the viscosity data (circles) at 0 °C for monodisperse PI chains in bulk[23] with the predictions of the CDCR (dash–dot curves) and CICR (dashed curves) models with the local jump gate numbers (z) as indicated. The other model parameters were determined from the experimental data through eqs 24 and 25.

Figures 11 and 12) suggests that a further modification of the CICR model (incorporation of some other relaxation mechanisms in addition to CR and reptation) never improves the agreement between the model and experiments: Such modifications always decrease the predicted viscosity.

In a previous work,[16] we have examined the dielectric behavior of *cis*-polyisoprene (PI) probe chains uniformly mixed and entangled only with polybutadiene (PB) matrices. The PI chains have dipoles aligned *parallel* to their contour.[18] Thus, in the PB matrices, two types of probe PI chains with and without inversion of dipole direction at the center of the contour exhibited the so-called *dielectric normal mode* relaxation due to end-to-center and end-to-end vector fluctuations, respectively.[16] For such PI chains, we found a universal dielectric mode distribution irrespective of the probe and matrix molecular weights.[16] In addition, for two types of PIs of nearly

the same length but with and without dipole inversion, the ratio of their dielectric relaxation times was insensitive to the matrix molecular weight.[16] These results were in agreement with the predictions of the CDCR model but were different even *qualitatively* from those of the CICR model.[17]

From the results found in this and previous work,[17] we conclude that the CICR model and any other models *leading to the factorized form of relaxation functions* (like μ given in eq 14) do not adequately describe the behavior of actual entangled systems. On the other hand, for both viscoelastic and dielectric relaxation, the CDCR model reasonably well describes the behavior of probe chains at least at *long* time scales. Thus, the dependence on chain configuration is quite likely essential for the relaxation rates of actual CR processes.

2. Problem for CDCR Model. For the CDCR model of the present form, we still have the following problem. In a previous work,[17] a CDCR model was formulated for a local correlation function:

$$C(n,t;m) = \langle \mathbf{u}(n,t)\cdot\mathbf{u}(m,0)\rangle/a^2 \qquad (27)$$

from which end-to-end and end-to-center correlation functions and thus dielectric relaxation functions of PI chains were calculated. (Here, $\mathbf{u}(n,t)$ is the nth bond of a probe chain at time t, and a is the segment size.) $C(n,t;m)$ contains the first-order moment with respect to $\mathbf{u}(n,t)$ at time t. This enabled us to formulate the CDCR model for $C(n,t;m)$ *rigorously* using Rouse dynamics as the CR dynamics,[17] as is different from the model for $S(n,t)$ incorporating DDA. Nevertheless, the model for $C(n,t;m)$ was good only for *terminal* dielectric relaxation and *underestimated* fast dielectric modes of probe PI chains. This result certainly indicates a limitation for the validity of Rouse dynamics in describing actual CR processes.[17] From this point of view, it is worthwhile to reexamine the validity of Rouse dynamics in a most critical way for blends in a *CR-dominant* regime.

In the *CR-dominant* regime, the CDCR model (for both $S(n,t)$ and $C(n,t;m)$) is identical with a *pure* CR model rigorously using the Rouse dynamics. As is characteristic of Rouse dynamics, the pure CR model for $S(n,t)$ predicts a universal dependence of the reduced modulus $G'_{L,B}M_L/\phi_L T$ on the reduced frequency $J_{L,B}\eta_{L,B}\omega$ (with $J_{L,B}\eta_{L,B}$ being the weight-average relaxation time). An experimental examination on this universality is a most critical test for the validity of Rouse dynamics. Figure 13 shows the results of this test on probe PS chains examined in this and previous work.[7-9]

In Figure 13, the reduced moduli of probe PS chains (with $M_w/M_n \leq 1.1$) entangled only with *much shorter* matrix PS chains are plotted against the reduced frequency (circles). The solid curve indicates the universal curve predicted from the pure CR model (eq 12 with $2D_t\lambda_q^2$ being replaced by $(\pi^2/15)q^2/J_{L,B}\eta_{L,B}$). We used eq 26 to correct the theoretical curves for the MWD of the probe PS chains, but it turned out that the small MWD ($M_w/M_n \leq 1.1$) hardly affected the predicted universality.

In Figure 13, we first note that the data points for various probe chains in various matrices are collapsed in a universal curve, as suggested from the pure CR model. In fact, this curve is close to the prediction of the model (solid curve) at low frequencies ($J_{L,B}\eta_{L,B}\omega \lesssim 10$). This result indicates the validity of Rouse dynamics for the *slow* CR processes in a most critical way. However, at short time scales ($J_{L,B}\eta_{L,B}\omega > 10$), we find a systematic deviation of the calculated $G'_{L,B}$ from the data. Clearly, high-order Rouse modes *overestimate* the fast viscoelastic CR relaxation to predict smaller $G'_{L,B}$ at high ω. We have again confirmed the limitation of Rouse dynamics.

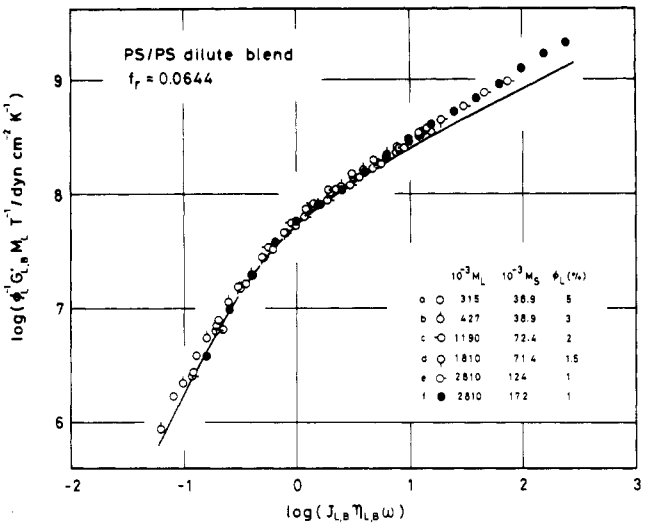

Figure 13. Plots of $G'_{L,B}M_L/\phi_L T$ against $J_{L,B}\eta_{L,B}\omega$ for probe PS chains entangled with much shorter PS matrices. The total polymer content ϕ_p is 100 vol % (bulk) for blends a (from ref 8), b, and c (both from ref 7) and 60 vol % for blends d (this work), e, and f (both from ref 9). The solid curve indicates the universal curve predicted by the pure CR model. The small MWD ($M_w/M_n \leq 1.1$) of the probe chains examined hardly affects the predicted universality.

Here we add some comments on why the present CDCR model for $S(n,t)$ reasonably well describes the viscoelastic data in spite of the limitation of Rouse dynamics used in the model. The Rouse and reptation eigenfunctions (f_{pq}^{CR} and f_p^{rep}; eqs 16 and 17) are not the same for $S(n,t)$ so that those of any mode order are coupled with one another when CR and reptation are competing. With increasing M_S ($\rightarrow M_L$) and decreasing CR contribution, the Rouse eigenfunctions of high orders become more importantly coupled with the low-order reptation eigenfunctions to describe terminal relaxation in the model. As found in Figure 13, high-order Rouse eigenfunctions overestimate fast viscoelastic modes of actual CR relaxation. At the same time, the diagonal dominance approximation (DDA) involved in the present model for $S(n,t)$ leads to an underestimation of those modes *as compared to the rigorous Rouse dynamics*.[21] Thus, the over- and underestimation seem to cancel with each other to some extent, possibly leading to reasonably good agreements between the model with DDA and slow viscoelastic data (Figures 8–10). In this connection, we expect that only removal of DDA from the model[21,24] does not necessarily improve the agreements with experiments.

The reasonable success of the CDCR model for $C(n,t;m)$ (for dielectric normal mode relaxation) was explained in the previous paper[17] as follows. This model rigorously uses Rouse dynamics as the CR dynamics. For $C(n,t;m)$, the Rouse and reptation eigenfunctions are the same and coupled in the model only when they have the same mode order. This fact enables the model to describe the slow dielectric relaxation in terms of *only* low-order Rouse and reptation eigenfunctions, those being valid for the terminal relaxation.

Finally, we briefly discuss a motion of a probe chain due to CR. In the present CDCR model, a Rouse motion is assumed in an a priori sense. In other words, we do not start from an explicit formulation for a fundamental local motion due to CR. In reality, some of the entanglement points for the probe chain would be removed by diffusion of the matrix chains during a certain period of time. Then

the probe chain should determine its motion by itself according to spatial arrangements of the removed and preserved entanglement points, and the diffusion of matrix chains is just a trigger for that motion. The resulting motion of the probe chain should be still approximated by a Rouse motion at long time scales as found in Figure 13, but not at short time scales. The Rouse dynamics over- and underestimates, respectively, the high-order viscoelastic and dielectric CR modes of actual systems. Formulation of the above molecular picture is an interesting and important work and will be addressed in a later paper.

VI. Conclusion

We have found that the slow viscoelastic relaxation of probe PS chains in PS/PS dilute blends was better described by the CDCR model than by the CICR model. The failure of the CICR model was also found in the previous work for dielectric relaxation of probe PI chains.[17] From these results we conclude that the configuration dependence is essential for actual CR processes and that the relaxation functions *factorized* into pure reptation and pure CR functions do not adequately describe the behavior of entangled systems.

The CDCR model describes the behavior of the probe chain reasonably well at long time scales but not at short time scales. The Rouse dynamics used in the model overestimates the fast (high order) viscoelastic CR modes (Figure 13). This in turn suggests that the reasonable success of the present model for the viscoelastic relaxation at long time scales may be related to the diagonal dominance approximation (DDA) used in the model. The DDA underestimates fast viscoelastic CR modes and seems to cancel to some extent the overestimation of those modes due to use of Rouse dynamics in the model.

References and Notes

(1) Ferry, J. D. *Viscoelastic Properties of Polymers*, 3rd ed.; Wiley: New York, 1980.
(2) Doi, M.; Edwards, S. F. *The Theory of Polymer Dynamics*; Clarendon: Oxford, 1986.
(3) Graessley, W. W. *Adv. Polym. Sci.* **1982**, *47*, 67.
(4) Doi, M. *J. Polym. Sci., Polym. Phys. Ed.* **1983**, *21*, 667.
(5) Klein, J. *Macromolecules* **1978**, *11*, 852.
(6) Daoud, M.; de Gennes, P.-G. *J. Polym. Sci., Polym. Phys. Ed.* **1979**, *17*, 1971.
(7) Watanabe, H.; Kotaka, T. *Macromolecules* **1984**, *17*, 2316.
(8) Watanabe, H.; Sakamoto, T.; Kotaka, T. *Macromolecules* **1985**, *18*, 1008, 1436.
(9) Watanabe, H.; Kotaka, T. *Macromolecules* **1986**, *19*, 2520.
(10) Watanabe, H.; Kotaka, T. *Macromolecules* **1987**, *20*, 530.
(11) Watanabe, H.; Kotaka, T. *J. Soc. Rheol. Jpn.* **1987**, *15*, 48.
(12) Watanabe, H.; Yoshida, H.; Kotaka, T. *Macromolecules* **1988**, *21*, 2175.
(13) Green, P. F.; Mills, P. J.; Palmstrøm, C. J.; Mayer, J. W.; Kramer, E. J. *Phys. Rev. Lett.* **1984**, *53*, 2145.
(14) Green, P. F.; Kramer, E. J. *Macromolecules* **1986**, *19*, 1108.
(15) Watanabe, H.; Tirrell, M. *Macromolecules* **1989**, *22*, 927.
(16) Watanabe, H.; Yamazaki, M.; Yoshida, H.; Adachi, K.; Kotaka, T. *Macromolecules*, in press.
(17) Watanabe, H.; Yamazaki, M.; Yoshida, H.; Kotaka, T. *Macromolecules*, in press.
(18) Adachi, K.; Kotaka, T. *Macromolecules* **1984**, *17*, 120.
(19) In ref 15, the CICR model was referred to as the extended Graessley model.
(20) (a) Doi, M.; Graessley, W. W.; Helfand, E.; Pearson, D. S. *Macromolecules* **1987**, *20*, 1900. (b) Rubinstein, M.; Helfand, E.; Pearson, D. S. *Macromolecules* **1987**, *20*, 822.
(21) See Appendix A of ref 15.
(22) According to the theory of rubber elasticity,[1] a small correction for the relaxation intensity ($\propto T$) was made. To this end, η for $\phi_p = 60$ and 36.4 vol % at T_r (with $f_r = 0.0644$) was multiplied by a factor T_r°/T_r and plotted against $\phi_p M$ in Figure 11. Here, T_r are the reference temperatures (in K) for $\phi_p = 60$ and 36.4 vol %, and T_r° is the T_r for $\phi_p = 100$ vol % (bulk). (We neglect here a minor correction for very small differences in the densities of the PS systems at the T_r's.)
(23) Adachi, K.; Yoshida, H.; Fukui, F.; Kotaka, T. *Macromolecules* **1990**, *23*, 3138.
(24) For viscoelastic relaxation, a CDCR model *without DDA* (rigorously using the Rouse dynamics as the CR dynamics) can be formulated for a function $S_2(n,m;t) = (1/a^2)\langle u_x(n,t)u_y(m,t)\rangle$ as[21,25]

$$\frac{\partial}{\partial t}S_2 = [D_t + D_c]\left[\frac{\partial^2}{\partial n^2} + \frac{\partial^2}{\partial m^2}\right]S_2 + 2D_c\frac{\partial^2}{\partial n \partial m}S_2$$

However, this equation (not solvable analytically) would not necessarily describe the behavior of actual systems better than the present model with DDA, because the overestimation for high-order CR modes due to use of rigorous Rouse dynamics is not canceled in the model without DDA.
(25) See note 37 of ref 15.

Registry No. PS, 9003-53-6.